Efficient Utilization of Higher-Lying Excited States to Trigger Charge-Transfer Events

Pierre-Antoine Bouit, Fabian Spänig, Gregory Kuzmanich, Evangelos Krokos, Christian Oelsner, Miguel a. Garcia-Garibay, Juan luis Delgado, Nazario Martín, Dirk m. Guldi

Efficient Utilization of Higher Lying Excited States to Trigger Charge Transfer Events

Pierre-Antoine Bouit,[a] Fabian Spänig,[c] Gregory Kuzmanich,[d] Evangelos Krokos,[c] Christian Oelsner,[c] Miguel A. Garcia Garibay,[d]* Juan Luis Delgado,[a,b] Nazario Martín,[a,b]* and Dirk M. Guldi.[c]*

(Dedicated to David I. Schuster on the occasion of his 75th birthday)

Abstract: Several new fullerene-heptamethine conjugates absorbing as far as 800 nm have been synthesized and fully characterized by physic-chemical means. In terms of optical and electrochemical characteristics appreciable electronic coupling between both electroactive species is deduced. The latter also reflects the excited state features. To this end, time resolved transient absorption measurements revealed that photoexcitation is followed by a sequence of charge transfer evolving from higher singlet excited states (i.e., S_2 – fast charge transfer) and the lowest singlet excited state (i.e., S_1 – slow charge transfer) of the heptamethine cyanine as electron donor to an either covalently linked C_{60} or C_{70} as electron acceptor. Finally, charge transfer from photoexcited C_{60} / C_{70} completes the charge transfer sequence. The slow internal conversion within the light harvesting heptamethine cyanine and the strong electronic coupling between the individual constituents are particularly beneficial.

Keywords: higher lying excited states · charge transfer ·near infrared dyes · fullerenes· heptamethine cyanine

Introduction

Natural systems able to transform efficiently sunlight into chemical energy through the photosynthetic processes, have inspired basic research and developments in the areas of photovoltaics [1] and photocatalysis.[2] Here, "light" reactions, where solar energy is harvested and converted into energy carriers, play a fundamental role. The successful mimicry of natural photosynthesis – involving the sequence of light harvesting, light funneling, charge separation, and charge shift – mandates the consideration of several aspects, that is, broad light harvesting and efficient charge separation, all combined with slow charge recombination.

For example, the delocalization of charges within the spherical carbon framework of C_{60} together with its rigid, confined structure of the aromatic π-sphere offers unique opportunities for stabilizing charged entities. Above all, the small reorganization energies of fullerenes in charge transfer reactions have led to a notable breakthrough in synthetic electron donor acceptor systems by providing accelerated charge separation and decelerated charge recombination. The vast majority of charge transfer reactions commences in the energetically low lying states. Ever since the pioneering work by Hammartström *et al*. reporting on the electron transfer from higher singlet excited states (i.e., S_2) of porphyrins to ruthenium (II) complexes,[3] follow-up studies on this topic have been published.[4] In these systems, the large energy gap existing between, for example, higher singlet excited states (i.e., S_2) and lowest singlet excited state (i.e., S_1) as well as the relatively long lifetime of S_2 emerged as key parameters. It is only been very recently that the possibility of designing optoelectronic switches has been forwarded – relying on electron transfer events that are triggered from different excited state precursors in metal-containing porphyrins.[5]

On the other hand, dealing with all organic electron donors, only a few examples have been published involving aromatic hydrocarbon containing systems.[6] In this regard, the relationship between structure and charge transfer reactivity will shape solar-to-energy conversion efficiencies, which makes it as important as any other parameter.

[a] Dr. P.-A. Bouit, Dr. J.L. Delgado, Prof. Dr. N. Martín
IMDEA-nanociencia, E-28049 Madrid, Spain.
Fax: +34 91394 4103; Tel: +34 91394 4227

[b] Dr. J.L. Delgado, Prof. Dr. N. Martín
Departamento de Química Orgánica,Facultad de C. C. Químicas,
Universidad Complutense de Madrid, 28040 Madrid (Spain)
Fax: (+34) 913944103
E-mail: nazmar@quim.ucm.es
Homepage: http://www.ucm.es/info/fullerene

[c] F. Spänig, E. Krokos, C. Oelsner, Prof. Dr. D. M. Guldi
Department of Chemistry and Pharmacy & Interdisciplinary Center of Molecular Materials (ICMM)
Friedrich-Alexander-University Erlangen-Nuremberg
Egerlandstr. 3, 91058 Erlangen, Germany
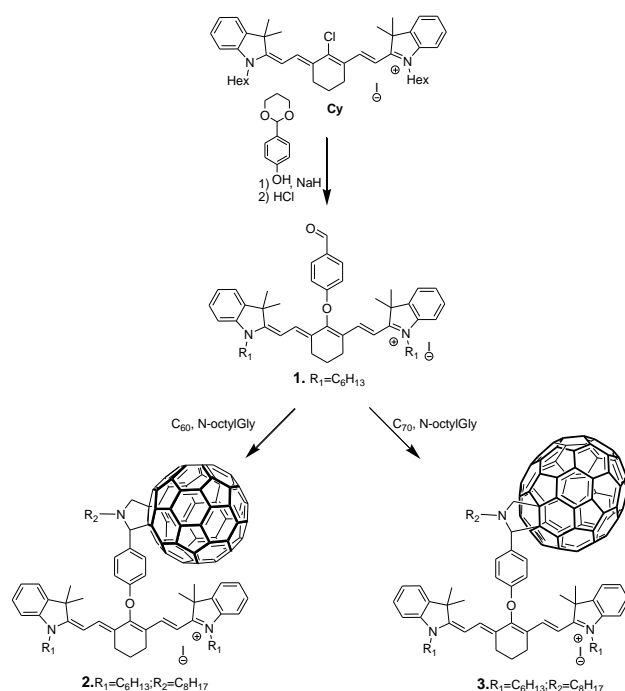E-mail: dirk.guldi@chemie.uni-erlangen.de

[d] G. Kuzmanich, Prof. Dr. M. A. Garcia Garibay
Department of Chemistry and Biochemistry
University of California
Los Angeles, California 90095-1569, USA
E-mail: mgg@chem.ucla.edu

Light harvesting, on the other hand, is rarely addressed, despite its paramount impact on organic photovoltaics. Extending the onset of light harvesting beyond 700 nm jeopardizes the charge transfer efficiency due to weak driving forces. Such a drawback can be partially compensated by lowering the redox potential of the photoactive components, which is, however, often accompanied by chemical instability. This calls for the necessity of higher lying excited states as a precursor for non-adiabatic charge transfer.

In the context of light harvesting in the infrared part of the solar spectrum, the exceptional optical properties of heptamethine cyanines are a great asset. Their stability is based on the delocalization of a positive charge between two amino end-groups through a rigid, odd-number $C(sp^2)$ carbon skeleton.[7] The complex electronic structure of heptamethine cyanines prompts to structural inertia and, in turn, to slow structural relaxation / thermalization, especially of higher excited states.[3b-d,4,8] All of the aforementioned criteria motivated us to probe them in conjunction with C_{60} as well as C_{70} as photo- and redox-active building blocks. Importantly – to the best of our knowledge – heptamethine cyanines covalently linked to fullerenes have never been probed in photoinduced charge transfer reactions neither as photo- nor as redox-active constituent.[9]

In this communication, we report on uncommon charge transfer evolving from higher singlet excited states of a heptamethine cyanine as electron donor to an either covalently linked C_{60} or C_{70} as electron acceptor. Beneficial is the slow internal conversion within the light harvesting heptamethine and the strong electronic coupling between the individual constituents.

Results and Discussion

Scheme 1. Synthesis of fullerene-heptamethine conjugates **2** and **3**

Synthesis The synthesis of the electron donor acceptor conjugates **2** and **3** was carried out in two steps starting from previously described heptamethine cyanines (**Cy**).[10] To this end, introducing *p*-hydroxybenzaldehyde to the chloro-heptamethine cyanine (**Cy**) was achieved by substitution of the meso-chlorine atom to form **1** (Scheme 1).[8a] Then, the reaction of **1** with either C_{60} or C_{70} in the presence of *N*-octylglycine,[11] afforded **2** and **3** as deep green solids in 40 % and 30 % yields, respectively. Notably, **3** was obtained and studied as a mixture of isomers due to the multiple possibilities of adding azomethine ylides to C_{70}.[12] Notably, the presence of various alkyl chains in **2** and **3** provides reasonable solubility to these compounds in common organic media. The structures of **2** and **3** were confirmed by ^{1}H and ^{13}C-NMR and high resolution MS experiments with molecular ion peaks for **2** ([M+H]$^+$ = 1555.6309 (calcd. $C_{118}H_{80}N_3O$: 1554.6296) and **3** [M+H]$^+$ = 1675.6292 (calcd. $C_{128}H_{80}N_3O$: 1674.6301) – see Figures S1 – S5 for details.

Optical properties The absorbance of **1** maximizes around 782 nm followed by weaker transitions in the blue region with maxima at 260, 387, and 440 nm (Figure 1). From this we calculated singlet excited state energies of ~3.0 and 1.55 eV. The spectra of **2** and **3** almost resemble the sum of the individual spectra, that is, **1** and either C_{60} or C_{70}. The well-known absorption bands of C_{60} and C_{70} are discernable at 256, 320, as well as 420 nm[13] and 236, 359, 377, 467, as well as 525 nm,[12,14] respectively. Evidence for electronic communication between the electron donor (i.e., **1**) and the electron acceptors (i.e., C_{60} and C_{70}) came from reduced extinction coefficients of **2** and **3** when compared to that of **1** (Figure 1).
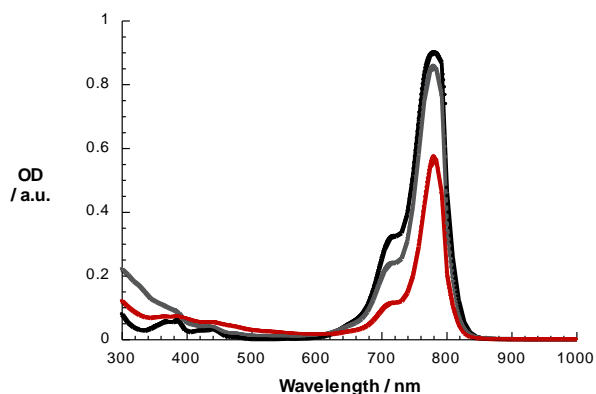
Figure 1. Absorption spectra of **1** (black spectrum), **2** (grey spectrum), and **3** (red spectrum) – 5.0 x 10^{-6} M – recorded in dichloromethane

Electrochemistry The electrochemical properties of **1**, **2**, and **3** have been studied in dichloromethane at room temperature by means of cyclic voltammetry (CV) and differential pulse voltammetry (DPV). As described for similar cationic heptamethines, **1** reveals an amphoteric redox character with a completely reversible one-electron reduction process at -1.02 V followed by a non reversible reduction process at -1.94 V versus ferrocene/ferricenium.[15] One-electron oxidation processes, on the other hand, are noted at +0.30 V – fully reversible – and +0.93 V – quasi reversible. Additionally, in **2** three reversible one-electron reduction processes – all centered at C_{60} – were observable at -1.18, -1.52, and -2.07 V (Figure 2). In **3**, one-electron reductions of C_{70} were detected at -1.20, -1.51, and -2.16 V. When compared to pristine C_{60}, these reduction potential values are cathodically shifted. Such a trend has been rationalized on the basis of saturating a double bond of C_{60}, which is known to rise the energy of the LUMO.[16,17] In both cases, namely **2** and **3**, the first oxidation of the cyanine was shifted cathodically to +0.20 V without, however, affecting the first reduction of **1** – see Figures S6 - S7. Consequently, we derive radical ion state pair energies of 1.38 eV (**2**) and 1.4 eV (**3**) in dichloromethane.
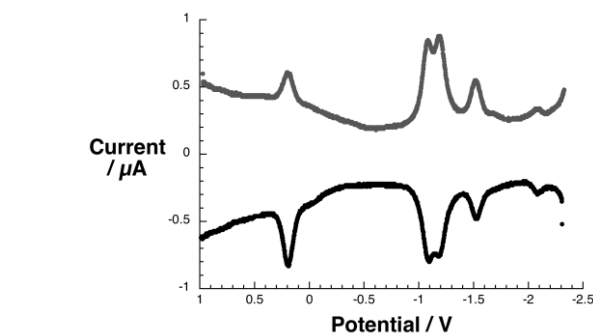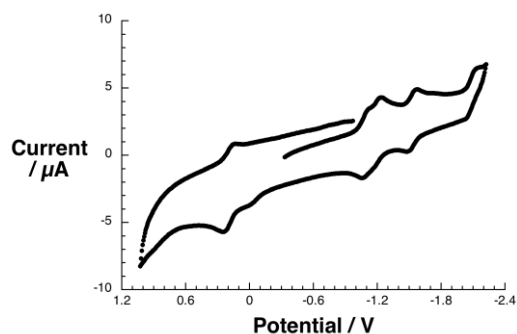

Figure 2. Upper part – cyclic voltammogram of **2** recorded in deaerated dichloromethane versus the ferrocene/ferricenium couple – TBAPF$_6$ was employed as supporting electrolyte. Lower part – corresponding differential pulse voltammogram.

Photophysical properties: Next, ultrafast laser flash photolysis experiments were carried out, employing either an excitation wavelength of 387 nm to photoactivate mainly C_{60} or C_{70} or an excitation wavelength of 775 nm to excite exclusively the cyanine moiety. Excitation of C_{60} and C_{70} at 387 nm populates their singlet excited states with characteristic absorption maxima at 610 / 920[11b-18] and 610 / 1360 nm (Figure S8),[19] respectively. The latter undergo intersystem crossing to the corresponding triplet manifolds with characteristic lifetimes of between 0.7 and 1.4 ns and characteristic maxima at 700 nm.[11b,18,20] The transient absorption spectra upon 387 nm excitation of **1** (Figure S9) in dichloromethane or benzonitrile are dominated by strong ground state bleaching at 800 nm. Directly upon laser excitation the higher singlet excited state features of **1** are discernable with maxima at 600, 850 and 940 nm, minima at 510, 565, 715, and 1255 nm, and broad bleach between 725 and 845 nm. With a lifetime of 2.6 ps these features transform rapidly into those of the lowest singlet excited state with distinct maxima at 515, 560, and 1250 nm plus distinct minima at 716 and 880 nm. The recovery of the ground state follows afterwards within 1650 ps. On the contrary, when 775 nm excitation is used (Figure S10) the lowest singlet excited state (1.56 eV) is formed instantaneously and rapidly (> 0.5 ps) bypassing any higher singlet excited states before converting to the triplet excited state.

When investigating **2** and **3**, instantaneously upon photoexcitation at 387 nm the higher singlet excited state features of **1** are discernable – *vide supra*.[21] Considering the time window, in which internal conversion and vibrational relaxation occurs for **1**, the transient characteristics in **2** and **3** start to transform in benzonitrile into main maxima at 600, 1015, and 1050 nm as well as 600, 850, 1015, and 1300 nm[11b,18,22] – the radical ion pair states. Support for this hypothesis was lent from a comparison with spectroelectrochemically and pulse radiolytically generated **1** radical dication. In fact, these are in perfect agreement with the transient maxima observed at 600 and 1050 nm. The transient features, on the other hand, at around 1015 and 850 / 1300 nm are in accordance with previous work by pulse radiolysis assigned to the C_{60} and C_{70} radical anions, respectively.[23] Following the charge separation (k_{CS1}), the charge recombination (k_{CR}) to recover the ground state sets in with a lifetime of 30 ps in **2** (Figure 4) and 45 ps in **3** (Figure S11).
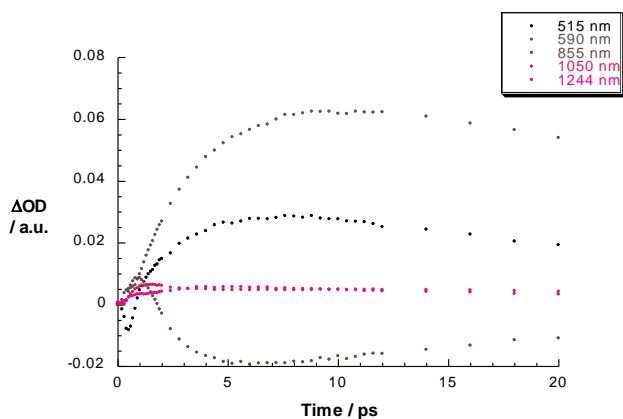
Figure 3. Upper part – differential absorption spectra (visible and near-infrared) obtained upon femtosecond flash photolysis (387 nm) of **2** in benzonitrile with several time delays between 0 and 10 ps at room temperature – time development from black to red to blue to orange and yellow. Lower part – time-absorption profiles of the spectra shown in the upper part at 515, 590, 855, 1050, and 1244 nm monitoring the competition between formation of the singlet excited state and charge separation as well as charge recombination.
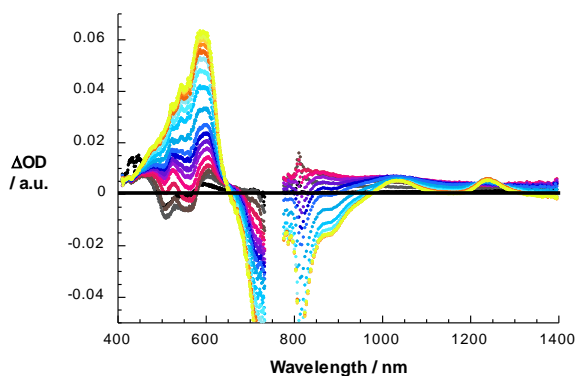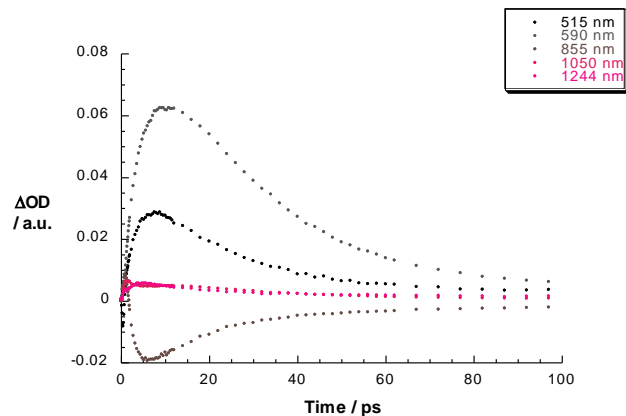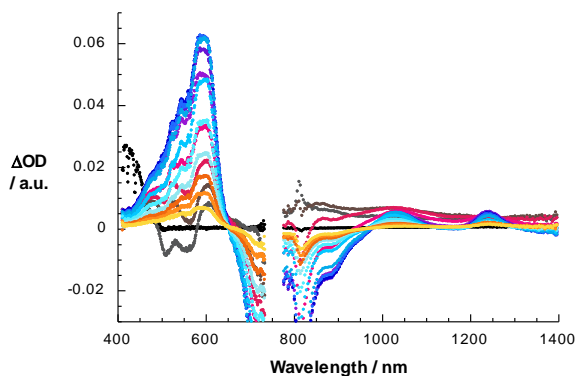

Figure 4. Upper part – differential absorption spectra (visible and near-infrared) obtained upon femtosecond flash photolysis (387 nm) of **2** in benzonitrile with several time delays between 0 and 100 ps at room temperature – time development from black to red to blue to yellow and yellow. Lower part – time-absorption profiles of the spectra shown in the upper part at 515, 590, 855, 1050, and 1244 nm monitoring the charge separation and charge recombination.

Notable is the competition between charge transfer – k_{CS1} – (i.e., 3.2 ps) and internal conversion / vibrational relaxation (i.e., 2.6 ps). The accordingly formed singlet excited states of **1** are discernable during the early times of our femtosecond experiments – shoulders at 515 and 560 nm plus the 1250 nm maximum. The latter reveals shortened lifetimes of 10 (**2**) and 14 ps (**3**) – k_{CS2} – in benzonitrile when compared to the intrinsic lifetime of **1** to generate the same radical ion pair state that originated from the higher singlet excited state – Figure 4. By decreasing the solvent polarity the lifetimes for charge separation and charge recombination in **2** (Figure S12) are extended to 3.5 and 14 ps, respectively. For **3** the lifetimes are 3.5 and 175 ps. Such lifetimes suggest charge separation (i.e., k_{CS1}, k_{CS2}) and charge recombination dynamics (i.e., k_{CR}) that are in the normal and inverted region of the Marcus parabola, respectively. In fact, a correlation between the charge transfer rate (i.e., charge separation and charge recombination) and the free energy change for the underlying reaction reveals a parabolic dependence – as illustrated in Figure 5 – with parameters of the reorganization energy (0.74 eV) and electronic coupling (89 cm^{-1}) closely resembling those seen in recent work involving C_{60}.
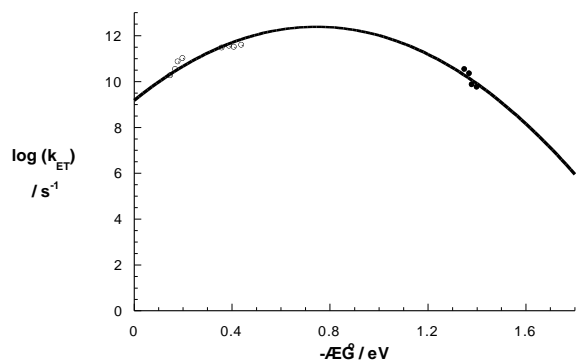
Figure 5. Driving force ($-\Delta G^0$) dependence of the rate constant for charge separation (open circles) and charge recombination (full circles).

Figure 6. Upper part – differential absorption spectra (visible and near-infrared) obtained upon femtosecond flash photolysis (778 nm) of **2** in benzonitrile with several time delays between 0 and 10 ps at room temperature – time development from black to red to blue to yellow and yellow. Lower part – time-absorption profiles of the spectra shown in the upper part at 515, 590, 855, 1050, and 1244 nm monitoring the competition between formation of the singlet excited state and charge separation as well as charge recombination.

When turning to the red, the singlet excited state features of C_{60} or C_{70} are discernable. In the case of C_{70}, these evolve in a region beyond where that of the heptamethine cyanine, namely 1350 to 1600 nm. Unlike what was seen for the reference systems the singlet excited state features are short-lived and transform into those of the radical ion pair states – vide supra. Multiwavelength analyses provide lifetimes in dichloromethane of 9 ps in **2** and 11 ps in **3**.

Upon exciting **2** (Figure 6) and **3** at 775 nm the directly and solely formed singlet excited state features, that is, maxima at 515, 560, and 1250 nm, are in contrast to **1** short-lived. In fact, they decay (k_{CS2}) in dichloromethane and benzonitrile with 30 and 10 ps (**2**) and 21 and 14 ps (**3**) to the radical ion pair states. Spectroscopically, the latter comprise for **2** maxima at 600, 1015, and 1050 nm, while **3** exhibits maxima at 600, 850, 1015, and 1300 nm. Remarkably good is the kinetic agreement – charge separation and charge recombination – between the 387 and 778 nm experiments.
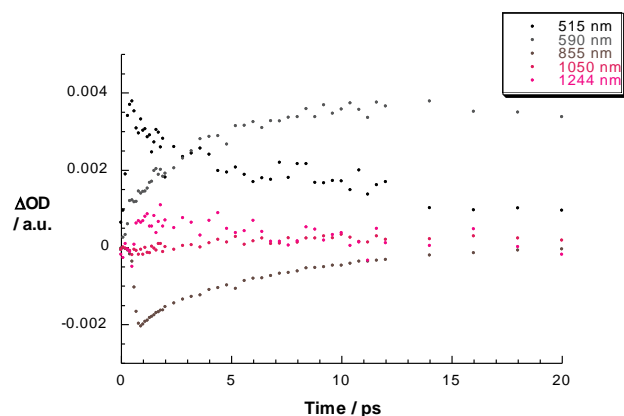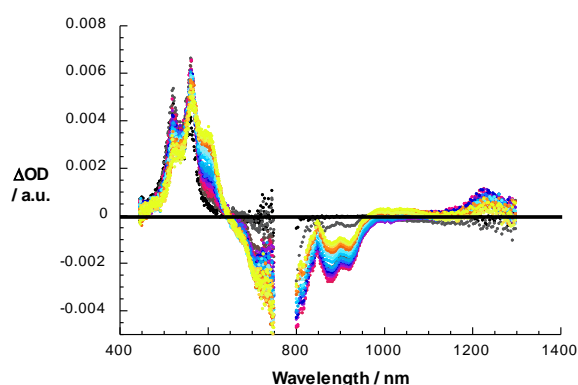
In summary, photoexciting at 387 nm in **2** or **3** with the prompt formation of higher singlet excited states results in two competing processes – Figure 7. On one hand, it is the charge separation that occurs with driving forces around 1.5 eV. Key to this pathway, is the close distance between the electron donor and the electron acceptor, which enables strong communication between them. On the other hand, it is the intrinsic deactivation to the lowest singlet excited state subject to a similar driving force. Considering the underlying kinetics, we estimate a branching of approximately 1 to 2. From the lowest singlet excited state we observe a charge transfer that is about 10 times slower ((k_{CS2}) = 30 ps (**2**) and 21 ps (**3**)) relative to the charge transfer that finds its origin in the higher singlet excited states ((k_{CS1}) = 3.2 ps (**2**) and 3.5 ps (**3**)). Decisive for the slower kinetics are driving forces of ca. 0.15 eV. The higher singlet excited state energies of 1.79 (C_{60}) and 1.76 eV (C_{70}) accelerates the charge separation (k_{CS3}) by increasing the driving force to nearly 0.4 eV in dichloromethane with 9 ps (**2**). It also opens new pathways for the recovery of the ground state, namely energy transfer.

Table 1. Charge separation and charge recombination rate constants for **2** and **3** in dichloromethane and benzonitrile.

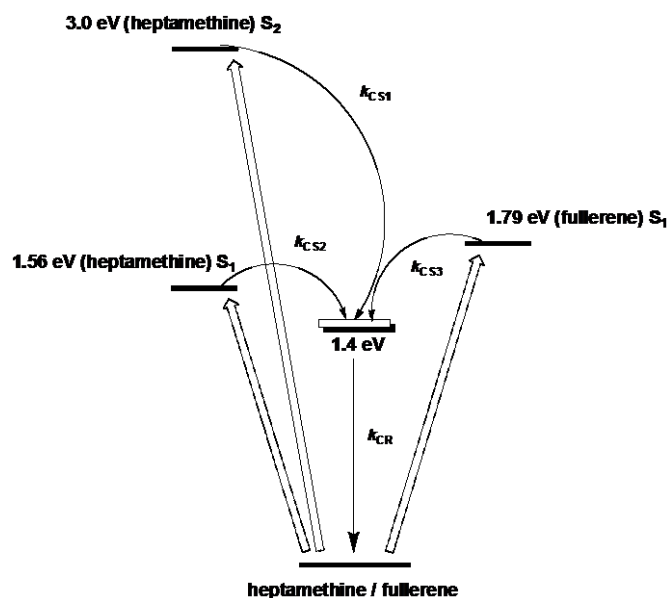|	solvent	k_{CS1}	k_{CS2}	k_{CS3}	k_{CR}
		10^{10} s^{-1}	10^{10} s^{-1}	10^{10} s^{-1}	10^{10} s^{-1}
2	dichloromethane	28.6	3.33	11.1	0.71
	benzonitrile	31.3	10.0		3.33
3	dichloromethane	28.6	4.76	9.1	0.57
	benzonitrile	34.5	7.14		2.22

5

Figure 7. Energy diagram illustrating the different excitation, charge separation (k_{CS1}, k_{CS2}, k_{CS3} – see for Table 1 for details), and charge recombination (k_{CR}) pathways in **2** and **3**.

Conclusions

The current investigation documents our success in realizing the rarely occurring scenario of a charge transfer commencing with a higher excited state through the tedious choice of electron donor and electron acceptor. In particular, the slow internal deactivation of excited state electron donating heptamethine cyanine and the acceleration of charge transfer reactions by the electron accepting C_{60} / C_{70} are crucial requisites. Currently, we are implementing heptamethine cyanines in multicomponent electron donor-acceptor conjugates to slow down charge recombination. From a broader perspective, we hope that this finding will provide the impetus for breakthroughs in near-infrared responsive photovoltaic devices.

Experimental Section

General synthetic procedures. NMR spectra (^{1}H, ^{13}C) were recorded at room temperature on Bruker DPX 300 MHz, Bruker AVIII. 500 MHz. Data are listed in parts per million (ppm) and are reported relative to tetramethylsilane (^{1}H, ^{13}C), residual solvent peaks being used as internal standard (CHCl$_3$ ^{1}H: 7.26 ppm, ^{13}C: 77.36 ppm, CDCl$_3$). High resolution mass spectrometry measurements were performed at the Unidad de Espectrometría de Masas of Universidad Complutense de Madrid. Column chromatography was performed on Merck 60 (40-63 µm) silica. Compound **Cy** was prepared according to published procedures.[5b]

Synthesis of 1. 4-(1,3-dioxan-2-yl)phenol (132 mg, 0.7 mmol, 1.1 eq.) is dissolved in DMF (20 mL) under argon atmosphere. NaH (19 mg, 1.2 eq.) is added. After 30 min of stirring at RT, this solution is added to **Cy** (500 mg, 0.66 mmol, 1 eq.) in DMF (20 mL). The solution is stirred 6 h at RT. The solution is then poured into ice and hydrochloric acid 1 M (200 mL). The resulting green solid is filtrated, dissolved in DCM and washed with water. The solution is then dried with MgSO$_4$ and evaporated. The crude is then dissolved in the minimum amount of DCM and precipitated in diethylether to afford a green solid (380 mg, 68 %). ^{1}H NMR (300 MHz, CDCl$_3$): 0.9 (t, J = 7 Hz, 6H); 1.1-1.5 (m, 14H); 1.63 (s, 12H); 1.7-1.8 (m, 4H); 2.0-2.1 (m, 2H); 2.7-2.8 (m, 2H); 4.12 (t, J = 7 Hz, 4H); 6.14 (d, J = 15 Hz, 2H); 7.05 (d, J = 8 Hz, 2H); 7.1-7.4 (m, 8H); 7.78 (d, J = 15 Hz, 2H); 7.97 (d, J = 8 Hz, 2H); 9.92 (s, 1H); ^{13}C NMR (75 MHz, CDCl$_3$): 4.9; 14.0; 21.0; 22.5; 24.6; 26.7; 27.3; 27.9; 31.4; 44.9; 49.0; 100.7; 110.8; 115.4; 122.0; 122.1; 125.2; 128.7; 131.3; 132.7; 141.0; 141.2; 142.2; 162.3; 164.0; 171.9; 190.6. MS (ESI+): [M]$^+$ = 709.6 (calcd. for C$_{49}$H$_{61}$N$_2$O$_2$: 709.5).

General procedure for the syntheses of 2 and 3: A solution of C$_{60}$ (130 mg, 0.18 mmol, 3 eq.) and *N*-octylglycine (11 mg, 1 eq) are refluxed in chlorobenzene (30 mL)

for 30 min Then, a solution of **1** (50 mg, 1 eq) in chlorobenzene (10 mL) is added dropwise during 2 h. The solution is refluxed 2 h more, and the solvent is evaporated. The crude is purified by column chromatography on silica gel (eluent: toluene then DCM-MeOH: 9-1). The resulting product is dissolved in the minimum amount of DCM and precipitated in pentane to afford a green solid (40 mg, 40 %). ^{1}H NMR (300 MHz, CDCl$_3$): 0.9 (t, J = 7 Hz, 9H); 1.1-1.5 (m); 1.7-1.8 (m); 2.0-2.1 (m, 2H); 2.4-2.6 (m, 1H); 2.7-2.9 (m, 4H); 3.0-3.1 (m, 1H); 4.12 (t, J = 7 Hz, 4H); 5.00 (s, 1H); 5.06 (d, J = 9 Hz , 1H); 6.10 (d, J = 15 Hz, 2H); 7.05 (d, J = 8 Hz, 2H); 7.1-7.4 (m, 8H); 7.85 (d, J = 15 Hz, 2H). ^{13}C NMR (125 MHz, CDCl$_3$): 14.4; 14.5; 15.6; 21.1; 22.4; 22.6; 24.5; 26.6; 27.2; 27.8; 27.9; 28.0; 28.3; 29.4; 29.7; 31.4; 31.9; 44.8; 48.8; 48.9; 53.4; 65.8; 66.6; 67.3; 68.9; 76.6; 81.9; 100.3; 110.7; 121.9; 122.5; 125.0; 126.4; 128.2; 128.5; 128.7; 129.0; 131.4; 134.2; 135.6; 136.0; 136.3; 137.2; 139.0; 139.8; 140.1; 140.2; 140.8; 141.2; 141.4; 141.5; 141.6; 141.7; 141.7; 141.8; 141.9; 142.0; 142.0; 142.1; 142.1; 142.2; 142.2; 142.3; 142.5; 142.5; 142.6; 142.7; 143.0; 143.1; 144.1; 144.3; 144.4; 144.7; 144.9; 145.0; 142.1; 145.3; 142.3; 145.3; 145.4; 145.5; 145.7; 145.8; 145.9; 146.0; 146.0; 146.1; 146.1; 146.2; 146.2; 146.3; 146.4; 146.5; 147.2; 147.3; 153.3; 153.4; 154.1; 156.6; 159.4; 163.5; 171.6; HRMS (MALDI+): [M+H]$^+$ = 1555.6309 (calcd. for C$_{118}$H$_{80}$N$_3$O: 1554.6296).

Compound **3** was synthesized using the same methodology, using C$_{70}$ as starting material to afford a green solid (30 %). HRMS (MALDI+): [M+H]$^+$ = 1675.6292 (calcd. for C$_{128}$H$_{80}$N$_3$O: 1674.6301).

Electrochemistry. Electrochemical experiments were carried out using a Princeton Applied Research Potentiostat/Galvanostat PAR 263A. Cyclic voltammetry, differential pulse voltammetry and square wave voltammetry were performed in a three electrode cell with a platinum wire as counter electrode, a glassy carbon disk as working electrode (Ø = 2 mm) versus a silver wire as reference electrode; ferrocene is applied as an internal standard and a 0.1 M solution of (*t*-Bu)$_4$NBF$_4$ as the supporting electrolyte. All experiments were performed under inert gas atmosphere and a compound concentration of 0.2 mM.

Spectroelectrochemistry: Spectroelectrochemical experiments were carried out using HEKA Elektronik Potentiostat/Galvanostat PG284 and a SPECORD S600 Analytic Jena Spectrophotometer. The measurements were performed in a homemade three neck cell (~ 0.3 cm) with a platinum gauze as working electrode, a platinum wire as counter electrode versus a silver wire under Argon atmosphere. Tetra-n-butylammonium hexafluorophosphate (Bu$_4$NPF$_6$ - 0.2 M) was used as supporting.

Photophysics. Steady State Fluorescence Spectroscopy: Horiba Jobin Yvon Fluoromax 3 spectrophotometer; in deaerated solution at room temperature (298 K) in a 1 to 1 cm quartz cuvette. All spectra were corrected for the instrument response. The monitoring wavelength was corresponding to the maximum of the emission band. Time Resolved Fluorescence: The fluorescence lifetime measurements were performed via time correlated single photon counting (TCSPC) by a FluoroLog-3 in T-configuration (HORIBA-JOBIN YVON) including a MCP detector (R3809U-58). Fluorescence lifetimes were measured at the emission maximum at room temperature in deaerated solution in a 1 to 1 cm quartz cuvette. fs-Transient Absorption Spectroscopy: Femtosecond transient absorption studies were performed with 775 and 387 nm laser pulses (1 kHz, 150 fs pulse width, 200 nJ) from an amplified Ti/sapphire laser system (Model CPA 2101, Clark-MXR Inc. – output 775 nm). The transient absorption pump probe spectrometer (TAPPS) Helios from Ultrafast systems is referred to as a two-beam setup, where the pump pulse is used as excitation source for transient species and the delay of the probe pulse is exactly controlled by an optical delay rail. As probe (white light continuum), a small fraction of pulses stemming from the CPA laser system was focused by a 50 mm lens into a 3-mm thick sapphire disc. The transient spectra were recorded using fresh oxygen free solutions in each laser excitation. All experiments were performed at 298 K in a 2 mm quartz cuvette. Pulse Radiolysis: Pulse radiolysis experiments were performed using 50 ns pulses of 15 MeV electrons from a linear electron accelerator (LINAC). Dosimetry was based on the oxidation of SCN$^-$ to (SCN)$_2$$^{\cdot-}$ which in aqueous, N$_2$O-saturated solution takes place with G ≈ 6 (G denotes the number of species per 100 eV, or the approximate µM concentration per 10 J absorbed energy). The radical concentration generated per pulse was varied between (1-3) × 10^{-6} M.

Acknowledgements

[1] For some very recent special issues, see: (a) Special issue on "*Organic Photovoltaics*", J.-L. Bredas, J. R. Durrant, eds. *Acc. Chem., Res.* **2009**, 42, 1689; (b) Special issue on "*Renewable Energy*", D. Nocera, D. M. Guldi, eds. *Chem. Soc. Rev* **2009**, *38*, 1; c) B. O'Regan, M. Grätzel, *Nature* **1991**, *353*, 737; d) S. Wenger, P.-A. Bouit,Q. Chen, J. Teuscher, D. Di Censo, R. Humphry-Baker, J. E. Moser, J.L Delgado, N. Martín, S. M. Zakeeruddin, M. Grätzel, *J. Am. Chem. Soc.* **2010**, *132*, 5164. e) S. Gunes, H. Neugebauer, N. S. Sariciftci, *Chem. Rev.* **2007**, *107*, 1324; f) B. C. Thompson, J. M. J. Frechet, *Angew. Chem. Int. Ed.* **2008**, *47*, 58; g) J. L. Delgado, P.-A. Bouit, S. Filippone, M.A. Herranz, N. Martín, *Chem. Commun.* **2010**, DOI: 10.1039/c003088k; e) I. Riedel, E. von Hauff, J. Parisi, N. Martín, F. Giacalone V. Diakonov, *Adv. Funct. Mater.* **2005**, 15, 1979.

[2] a) N. Armaroli, V. Balzani, *Angew. Chem. Int. Ed.* **2007**, *46*, 52; A. Fihri, V. Artero, M. Razavet, C. Baffert, W. Leibl, M. Fontecave, M. *Angew. Chem., Int. Ed.*, **2008**, *47*, 564.

[3] D. LeGourrierec, M. Andersson, J. Davidsson, E. Mukhtar, L. Sun, L. Hammarstrom, *J. Phys. Chem. A* **1999**, *103*, 557.

[4] a) N. Mataga, H. Chosrowjan, Y. Shibata, N. Yoshida, A. Osuka, T. Kikuzawa, T. Okada, *J. Am. Chem. Soc.* **2001**, *123*, 12422; b) T. Kesti, N. Tkachenko, H. Yamada, H. Imahori, S. Fukuzumi, H. Lemmetyinen, *Photochem. Photobiol. Sci.* **2003**, *2*, 251; c) J. Petersson, M. Eklund, J. Davidsson, L. Hammarström, *J. Am. Chem. Soc.* **2009**, *131*, 7940.

[5] S. Wallin, C. Monnereau, E. Blart, J.-R. Gankou, Fabrice Odobel, Leif Hammarström, *J. Phys. Chem A* **2010**, *114*, 1709.

[6] a) P.-A. Muller, E. Vauthey, *J. Phys. Chem. A* **2001**, *105*, 5994; b) M. Sakamoto, X. Cai, M. Hara, M. Fujitsuka, T. Majima, *J. Am. Chem. Soc.* **2004**, *126*, 9709.

[7] a) R. S. Lepkowicz, O. V. Przhonska, J. M. Hales, J. Fu, D. J. Hagan, E. W. Van Stryland, M. V. Bondar, Y. L. Slominsky, A. D. Kachkovski, *Chem. Phys.* **2004**, *305*, 259. b) P.-A. Bouit, C. Aronica, L. Toupet, B. Le Guennic, C. Andraud, O. Maury *J. Am. Chem. Soc.*, **2010**, *132*, 4328.

[8] a) R. S. H. Liu, A. E. Asato, *J. Photochem. Photobiol. C* **2003**, *4*, 179; b) N. Mataga, S. Taniguchi, H. Chosrowjan, A. Osuka, N. Yoshida, *Photochem. Photobiol. Sci.* **2003**, *2*, 493; c) M. Sakamoto, X. Cai, M. Hara, S. Tojo, M. Fujitsuka, T. Majima, *J. Phys. Chem. A* **2004**, *108*, 10941; d) M. Kubo, Y. Mori, M. Otani, M. Murakami, Y. Ishibashi, M. Yasuda, K. Hosomizu, H. Miyasaka, H. Imahori, S. Nakashima, *J. Phys. Chem. A* **2007**, *111*, 5136.

[9] For example of systems with smaller trimethine cyanine and C_{60} showing weak photovoltaic properties, see: F. Meng, J. Hua, K. Chen, H. Tian, L. Zuppiroli, F. Nuesch, *J. Mater. Chem.* **2005**, *15*, 979.

[10] a) N. Narayan, G. J. Patonay, *J. Org. Chem.* **1995**, *60*, 239; b) P.-A. Bouit, G. Wetzel, G. Berginc, L. Toupet, P. Feneyrou, Y. Bretonnière, O. Maury, C. Andraud, *Chem. Mater.* **2007**, *19*, 5325.

[11]a) M. Maggini, G. Scorrano, M. Prato, *J. Am. Chem. Soc.* **1993**, *115*, 9798; b) M. Prato, M. Maggini, *Acc. Chem. Res.* **1998**, *31*, 519; c) N. Tagmatarchis, M. Prato, *Synlett* **2003**, 768.

[12] a) A. Hirsch, M. Brettreich, in *Fullerenes*, Wiley-VCH, Weinheim, Germany, 2005. b) J.L. Delgado, E. Espíldora, M. Liedtke, A. Sperlich, D. Rauh, A. Baumann, C. Deibel, V. Dyakonov, N. Martín, *Chem. Eur. J.*, **2009**, *15*, 13474.

[13] a) S. Leach, M. Vervloet, A. Desprès, F. Bréheret, J. P. Hare, T. J. Dennis, H. W. Kroto, R. Taylor, D. R. M. Walton, *Chem. Phys.* **1992**, *160*, 451; b) D. M. Guldi, K.-D. Asmus, *J. Phys. Chem. A* **1997**, *101*, 1472.

[14] H. Ajie, M. M. Alvarez, S. J. Anz, R. D. Beck, F. Diederich, F. K., D. R. Huffman, W. Krätschmer, Y. Rubin, K. E. Schriver, D. Sensharma, R. L. Whetten, *J. Phys. Chem. A* **1990**, *94*, 8630.

[15] P.-A. Bouit, D. Rauh, S. Neugebauer, J. L. Delgado, E. Di Piazza, S. Rigaut, O. Maury, C. Andraud, V. Dyakonov, N. Martín, *Org. Lett.* **2009**, *11*, 4806.

[16] L. Echegoyen, and L.E. Echegoyen, *Acc. Chem. Res.* **1998**, *31*, 593.

[17] a) N. Martín, L. Sanchez, B. Illescas, and I. Perez, *Chem. Rev.* **1998**, *98*, 2527. b) N. Martín, *Chem. Commun.* **2006**, *2093.* c) N. Martin, L. Sanchez, M. A Herranz, B. M. Illescas, D. M. Guldi, *Acc. Chem. Res.* **2007**, *40*, 1015; d) F. Giacalone, J. L. Segura, N. Martin, N.; D. M. Guldi, *J. Am. Chem.Soc.* **2004**, *126*, 5340; e) M. A. Herranz, N. Martin, S. Campidelli, M. Prato, G. Brehm, D. M. Guldi, *Angew. Chem. Int. Ed*. **2006**, 45, 4478; f) M. Wielopolski, C. Atienza, T. Clark, D. M. Guldi, N. Martin, *Chem. Eur. J*. **2008**, 14, 6379. g) S. S. Gayathri, M. Wielopolski, E. M. Perez, F. Fernandez, G.; L. Sanchez, R. Viruela, E. Orti, E.; D. M. Guldi, N. Martin, N. *Angew. Chem., Int. Ed.* **2009**, *48*, 815; h) A. Molina-Ontoria, G. Fernandez, M. Wielopolski, C. Atienza, L. Sanchez, A. Gouloumis, T. Clark, N. Martin, N. ; D. M. Guldi, *J. Am. Chem. Soc* **2009**, 131, 12218. i) B. M. Illescas, J. Santos, M. Wielopolski, C. M. Atienza, N. Martin, D. M. Guldi, *Chem. Commun*. **2009**, 5374.

[18] D. M. Guldi, F. Hauke, A. Hirsch, *Res. Chem. Intermed.* **2002**, *28*, 817.

[19] C. S. Foote, *Top. Curr. Chem.* **1994**, *169*, 347.

[20] M.R. Fraelich, R. B. Weisman, *J. Phys. Chem.* **1993**, *97,* 11145.

[21] Approximate absorption ratio between C_{60} / C_{70} and the heptamethine cyanine is 9:1.

[22] C. A. Reed, R. D. Bolskar, *Chem. Rev*. **2000**, *100*, 1075.

[23] G. H. Sarova, U. Hartnagel, D. Balbinot, S. Sali, N. Jux, A. Hirsch, D. M. Guldi, *Chem. Eur. J.* **2008**, *14*, 3137.